Electrochimica Acta 108 (2013) 241–247

Contents lists available at ScienceDirect

Electrochimica Acta

journal homepage: www.elsevier.com/locate/electacta

The improvement of catalytic efficiency by optimizing Pt on carbon cloth as a cathode of a microbial fuel cell

S.J. Yen[a], M.C. Tsai[b], Z.C. Wang[c], H.L. Peng[c], C.H. Tsai[b], T.R. Yew[a,*]

[a] Department of Materials Science and Engineering, National Tsing-Hua University, Hsinchu 30013, Taiwan
[b] Department of Engineering and System Science, National Tsing-Hua University, Hsinchu 30013, Taiwan
[c] Department of Biological Science and Technology, National Chiao-Tung University, Hsinchu 30013, Taiwan

ARTICLE INFO

Article history:
Received 8 April 2013
Received in revised form 31 May 2013
Accepted 1 June 2013
Available online 24 June 2013

Keywords:
Cathode
Electrodeposition
Pt loading
MFC

ABSTRACT

This paper presents the performance of Pt deposited by different deposition methods, including electrodeposition, e-gun, and sputtering on a carbon cloth as a cathode in a microbial fuel cell (MFC) system. The results indicate that Pt deposited by electrodeposition exhibits the highest active efficiency on hydrogen electroabsorption. According to XPS fitting results, the amount of Pt (0), zero-valent Pt, existing in Pt deposited on carbon cloth by electrodeposition was larger than that in Pt deposited by e-gun and sputtering. The cyclic voltammogram analyses also show more real active surface area of Pt deposited by electrodeposition, mostly contributed by its smaller particle size/shape and higher catalytic effect. Besides, the total impedance of Pt deposited by electrodeposition was lower than that of Pt deposited by e-gun and sputtering from EIS measurement at 0.1 Hz. Applied to MFC system, the highest power density was manifested and the least Pt loading were observed for the Pt deposited on carbon cloth by electrodeposition. It is therefore can be concluded that the electrodeposited-Pt exhibit superior performance as a cathode for future MFC applications.

1. Introduction

Microbial fuel cells (MFCs) are gaining acceptance as an alternative energy technology in addition to the traditional environmental energy sources such as solar, wind and geothermal power [1]. MFCs also emerged as potential sustainable biotechnological solutions to future energy needs [2,3] and provided an innovative technology to recover electric energy from organic matters [4]. Bacteria were used in MFCs to catalyze the conversion of organic matter to electricity directly without the need of metal catalysts at the anode. Besides, the bacteria biologically oxidize organic matter and transfer electrons to the anode [5,6].

Many studies have mentioned that the cathode also plays a critical role on the performance of MFCs [7–9]. The cathode materials which exhibit a high redox potential are easy to capture protons. Currently, the common cathode materials are graphite, carbon cloth, and carbon paper [9]. In many MFCs, precious metals such as Pt, Pd [8,10] and other materials such as FePc, MnO_2 [11,12] were used as a catalyst. For example, Birry et al. [10] reported the use of FePc-based catalysts as a cathode in a pyrolyzed process at a high temperature and demonstrated its stable performance after a long-term MFC operation. Zhang et al. [13] and Zhang et al. [14] used iron-tetrasulfophthalocyanine (FeTsPc) as a cathodic catalyst to achieve a maximum power density of 817 mW/m^2, which was close to the value of 856 mW/m^2 using Pt as a catalyst on carbon cloth.

Zhang et al. [15] reported three kinds of manganese dioxides, including α-MnO_2, β-MnO_2, and γ-MnO_2, as a cathodic catalyst for MFCs with high activity. This study also suggested that β-MnO_2 exhibited a high potential to improve the feasibility of scaling up MFCs for real applications. Mahmoud et al. [16] reported the use of spinel manganese–cobalt (Mn–Co) oxide as a catalyst for MFCs. In this study, Mn–Co catalyst was oxidized with 2 at% of Mn and Co to generate high power, though still with a value lower than that of Pt catalyst. Hrapovic et al. [17] and Selembo et al. [18] reported the use of Ni particles or Ni powders as a cathodic catalyst in MFCs, showing similar performance compared to Pt powders in MFC system. Ni powders were demonstrated to be stable during 12 days MFC operation. The use of wet-proof nickel foam as a cathodic electrode in MFCs has been reported by Liu et al. [19] The results indicated that the wet-proofing was a promising method to enhance the stability and performance of metal cathodic electrode in MFCs.

Wang et al. [8] developed an iron-chelated catalyst for MFCs, which was prepared by pyrolyzed carbon (C) mixed with iron-chelated ethylenediaminetetraacetic acid (PFeEDTA/C) in an argon atmosphere. The results showed that the PFeEDTA/C was stable

* Corresponding author at: Department of Materials Science and Engineering, National Tsing-Hua University, 101, Sec. 2, Kuang-Fu Road, Hsinchu 30013, Taiwan. Tel.: +886 936347230; fax: +886 3 5722366.
E-mail address: tryew@mx.nthu.edu.tw (T.R. Yew).

0013-4686/$ – see front matter © 2013 Elsevier Ltd. All rights reserved.
http://dx.doi.org/10.1016/j.electacta.2013.06.019

during an operation period of 31 days. Kim et al. [20] used Co-napththalocyanine (Co-NPc) as a cathodic catalyst for MFCs and showed that it could improve catalytic activity over carbon. Yu et al. [21] reported the use of metal tetramethoxyphenylporphyrin (TMPP) and cobalt tetramethoxyphenylporphyrin (CoTMPP) as MFC cathodic catalysts. These catalysts were demonstrated to exhibit high activity and high power density in MFC system, showing their potential to replace Pt catalyst. However, many studies have mentioned that Pt as a cathodic catalyst revealed high electrochemical activity and stability. Pt as a cathodic catalyst still showed better performance than that of other types of catalysts so far [22–24]

The study is to improve the catalytic efficiency of Pt deposited on carbon cloth as a cathode in a MFC system. The different deposition methods such as electrodeposition, e-gun, and sputtering were adapted for this purpose. It is the first time to compare different deposition methods of Pt catalyst for the application in the MFC system. The effect of different Pt loading versus power density was also studied. Various electrochemical and physical characterizations on Pt catalysts were carried out, including scanning electron microscopy (SEM), grazing incident X-ray diffractometer (GIXRD), cyclic voltammogram (CV), X-ray photoelectron spectroscopy (XPS), and inductive coupled plasma-mass spectroscopy (ICP-MS) to examine the performance of Pt as a cathodic catalyst.

2. Materials and methods

2.1. Electrode preparation

A carbon cloth (CC) (1 cm × 1 cm) purchased from ElectroChem Inc. was used as an anode for the MFC system. Multi-walled carbon nanotubes (MWCNTs) were synthesized by chemical vapor deposition (CVD) on carbon cloth (MWCNTs/CC) at 800 °C according to the process that Tsai et al. [26] reported. The MWCNTs/CC was treated by nitric acid (Scharlau, 65%) at 80 °C for 12 h, washed by deionized (DI) water, and then dried at 120 °C in oven so as to provide hydrophilic surface to be used in the anode. A Cu/Ni wire (1 mm in diameter) applied with Ag gel was inserted in the MWCNTs/carbon cloth for external circuit connection.

The cathode of the MFC was composed of a piece of carbon cloth deposited with Pt. There were three different methods to deposit Pt on carbon cloth, including electrodeposition, e-gun, and sputtering. The carbon cloth was treated with nitric acid (named as a-CC) at 80 °C for 24 h before Pt deposition. For the e-gun deposition, the deposition rate was controlled at 0.1–0.2 Å/s at a deposition temperature less than 100 °C. For the sputtering of Pt, the deposition rate was 0.75 Å/s at a deposition temperature of about 30 °C. After a series of investigation, the optimized thickness of Pt was achieved at 420 nm for e-gun deposition and 700 nm for sputter system (see supplementary information Table S1). For electrodeposition, the deposition process is illustrated in the next paragraph with the optimized condition shown in supplementary information Table S2.

A three-electrode electrochemical cell was used for Pt electrodeposition. Pt nanoparticles were deposited on carbon cloth via a pulse-mode potentiostatic approach at a high potential of 0 V_{SCE} and a low voltage of −1.2 V_{SCE}. A saturated calomel electrode (SCE) was used as a reference electrode with a Pt mesh serving as a counter electrode. To achieve a larger driving force for the reduction of Pt metal ions onto the surface of carbon cloth by electrodeposition, 0.5 mM $H_2PtCl_6{\cdot}6H_2O$ (Alfa Aesar®, item #11051) was formulated in aqueous citric acid (CA) solution (0.15 M) as a precursor. The electrolytes were saturated with Ar atmosphere during deposition processes conducted at 760 Torr with a controlled temperature of ∼30 °C and magnetic stirring. After a series of process optimization, the Pt catalyst was electrodeposited at a fixed holding time of 0.2 s at −1.2 V_{SCE} and 2.5 s at 0 V_{SCE} for 111 cycles (see the supplementary information Table S2). Afterwards, the Pt deposited by electrodeposition (ed-Pt), e-gun (eg-Pt) and sputtering (sp-Pt) was annealed at 500 °C under Ar ambient at 1.5 Torr in a furnace. An Autolab PGSTAT302N potentiostat was employed for all electrochemical operations (Tsai et al. [25]).

2.2. Bacteria growth

The *Escherichia coli* (*E. coli*) (strain DH5α) (FRIDI, Taiwan) were used in this work. The strain DH5α was grown aerobically in a 50 ml bottle in Luria-Bertani (LB) broth. This culture was incubated on to anode at 37 °C, shaking at 200 rpm for 18 h. The cathode with Pt deposited on acid-treated carbon cloth (Pt/a-CC) was then put into the DH5α/LB solution. Finally, the MFC was fabricated to measure the polarization curves. Except *E. coli*, all equipments used in the experiment were sterilized for 30 min before put to use in order to prevent the contamination of MFC system from other bacteria.

2.3. Characterization

A single-chamber MFC system (Fig. 1a) was setup to measure the anode and cathode polarization curves. Polarization curves were measured using a potentiostat (Autolab, PGSTAT302N) at a scan rate of 10 mV/s. X-ray photoelectron spectroscopy (XPS) was used to characterize the chemical oxidation state of Pt surface. The morphology and structure of Pt/a-CC cathodes were analyzed by a scanning electron microscopy (SEM, JEOL 6500) and grazing incident X-ray diffractometer (GIXRD) (Rigaku, Cu Kα source, λ = 1.54056 Å).

A conventional three-electrode test cell was used for electrochemical measurements. The changes of the impedance of ed-Pt, eg-Pt, and sp-Pt on carbon cloth were measured by electrochemical impedance spectroscopy (EIS) (Autolab, PGSTAT302N). The 10 mV sinusoidal signals at various frequencies (0.1–100 kHz) were applied to the cathode of carbon cloth deposited with Pt in LB/DH5α solution. The cyclic voltammogram (CV) was also employed to evaluate the electrochemical property of cathodes using a potentiostat (Autolab, PGSTAT302N) in 0.5 M H_2SO_4 solution. In CV-test, the Pt cathode was used as a working electrode, Pt mesh as a counter electrode, and Ag/AgCl as a reference electrode. The potential was varied from −0.25 V to 1.0 V (vs. standard hydrogen electrode, SHE) with a scan rate of 50 mV/s. The amount of deposited-Pt (i.e. Pt-loading) was measured by an inductively coupled plasma-mass spectrometer (ICP-MS, SCIEX ELAN 5000).

3. Results and discussion

3.1. Surface characterization of carbon cloth, a-CC, and various Pt/a-CC

The Pt deposited on carbon cloth was analyzed by X-ray photoelectron spectroscopy (XPS). The XPS spectra in Fig. 1b and c provide the evidence of carboxylic-group bonding on the surfaces of pristine carbon cloth (CC) and acid-treated carbon cloth (a-CC), respectively. The C 1s XPS spectrum can be fitted to four Gaussian–Lorentzian peaks, which are contributed by sp2 hybridized carbons sp2-C (∼284.5 eV), hydroxyls or phenol C—OH or C—O (∼286 eV), carbonyl C═O (∼287 eV), and carboxyl HO—C═O (∼288.5 eV) [26–28]. These figures show that the total percentage of C—O or C—OH, C═O and HO—C═O bondings in carbon cloth after acid-treatment is higher than that of pristine carbon cloth. It indicates that the formation of hydrophilic chemical bonds such as C—O or C—OH, C═O and OH—C═O on the outermost surface of the carbon cloth [29] has been enhanced by acid treatment.

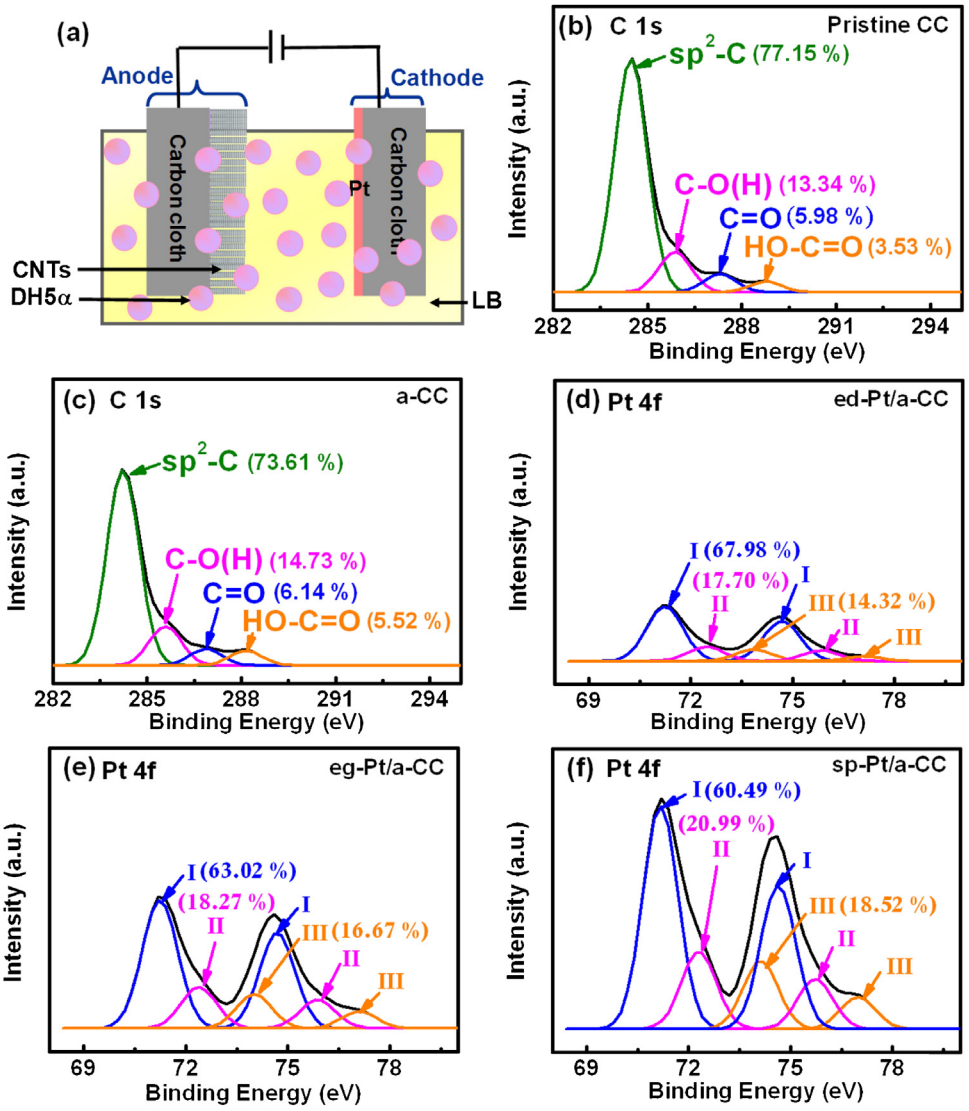

Fig. 1. Scheme of MFC set-up was showed in (a). XPS analyses showing (b) C 1s spectrum of pristine carbon cloth, (c) C 1s spectrum of a-CC, and the Pt 4f spectra of the Pt deposited on acid-treated carbon cloth by (d) electrodeposition, (e) e-gun, and (f) sputtering. The three pairs, labeled as I, II, III of doublets, are contributed by metallic Pt (0), Pt (II), and Pt (IV), respectively.

Fig. 1d–f shows the Pt 4f XPS spectra of Pt deposited on carbon cloth by electrodeposition (ed-Pt/a-CC), e-gun (eg-Pt/a-CC) and sputtering (sp-Pt/a-CC), respectively. The Pt4f signal consisted of three pairs, labeled as I, II, III, after deconvolution of doublets. The most intense doublet (71.2 and 74.6 eV) is contributed by metallic Pt (0) (zero-valent Pt). The second doublet (72.4 and 75.7 eV), with a binding energy (BE) of about 1.2 eV higher than Pt (0), could be assigned to Pt (II) (two-valent Pt) chemical state in PtO and $Pt(OH)_2$. The third doublet (74.1 and 77.1 eV) is mostly attributed to Pt (IV) (four-valent Pt) sate in PtO_2 [30–32]. Table 1 summarizes the binding energies of 71.2, 72.4, and 74.1 eV and their respective relative intensities. The intensities of components I, II, and III are 67.98%, 17.70%, 14.32% for ed-Pt/a-CC, 63.02%, 18.27%, 16.67% for eg-Pt/a-CC and 60.49%, 20.99%, 18.52% for sp-Pt/a-CC samples, respectively. The results indicate that the amount of Pt (0) of ed-Pt (67.98%) is higher than that of eg-Pt (63.02%) and sp-Pt (60.49%).

The higher amount of Pt (0) in ed-Pt may play an important role in this case. From the XPS fitting results, the components I, II, and III represent Pt (0), Pt (II), and Pt (IV) amounts on Pt surface, respectively [33,34]. The amount of Pt (0) for ed-Pt (67.98%) on carbon cloth is larger than that of eg-Pt (63.02%) and sp-Pt (60.49%). According to the catalytical effect of Pt, Pt (0) exhibits the best catalytic effect and provides highest active efficiency for hydrogen electroabsorption [35–37]. Pt (II) is a semi-stable state which reveals low catalytic effect, and Pt (IV) is almost an oxidative state without catalytic effect [34–36]. The sample with ed-Pt increased the Pt (0) amount by 5% and 7% more than that of eg-Pt and sp-Pt, respectively, which may explain why the ed-Pt as a cathodic catalyst exhibits higher activity for MFC applications.

Table 1
The relative intensities of components I (Pt (0)), II (Pt (II)), and III (Pt (IV)) for the Pt deposited on acid-treated carbon cloth by electrodeposition, e-gun and sputtering, which were calculated from XPS spectra.

Methods of Pt deposition	Relative intensity of species (%)		
	I	II	III
Electrodeposition	67.98	17.70	14.32
E-gun	63.02	18.27	16.67
Sputtering	60.49	20.99	18.52

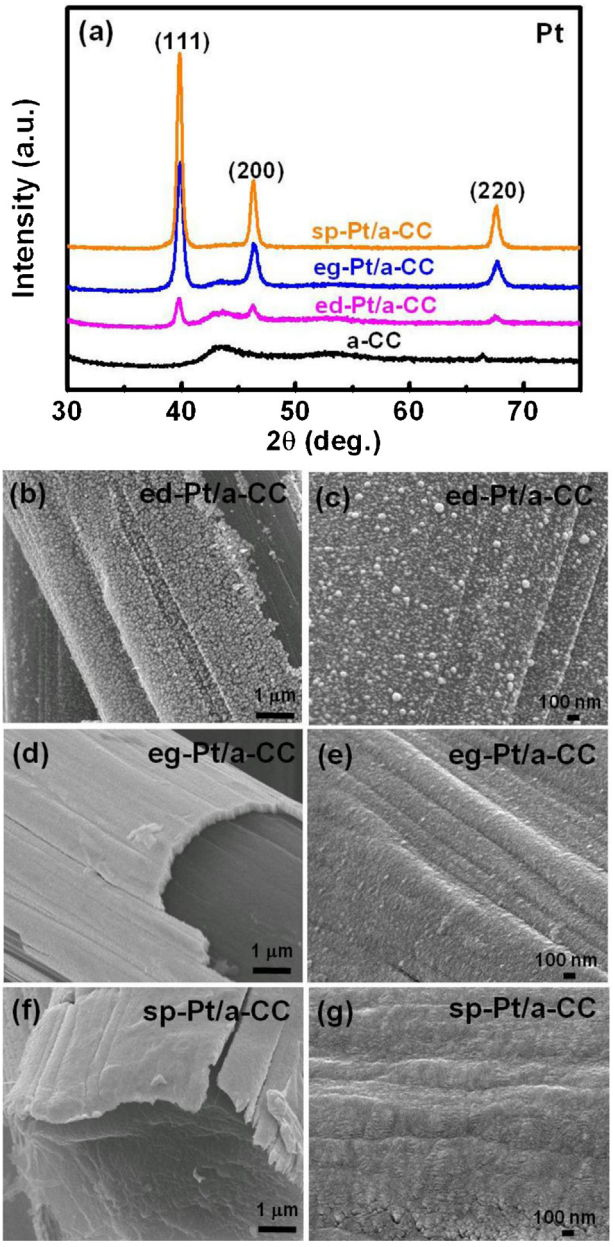

Fig. 2. XRD patterns of a-CC, and the Pt deposited by electrodeposition (ed-Pt), e-gun (eg-Pt), and sputtering (sp-Pt), on acid-treated carbon cloth (a-CC) were showed in (a). SEM images of Pt deposited on acid-treated carbon cloth (a-CC) by electrodeposition (ed-Pt/a-CC) at (b) low and (c) high magnifications, by e-gun (eg-Pt/a-CC) at (d) low and (e) high magnifications, and by sputtering (sp-Pt/a-CC) at (f) low and (g) high magnifications, respectively.

3.2. Structure and morphology of Pt/a-CC

Crystallinities of the ed-Pt, eg-Pt, and sp-Pt on acid-treated carbon cloth (i.e., ed-Pt/a-CC, eg-Pt/a-CC, and sp-Pt/a-CC, respectively) were investigated by GIXRD, with the results shown in Fig. 2a. The 2θ peaks of Pt (1 1 1), Pt (2 0 0), and Pt (2 2 0) were observed at 39.8°, 46.3°, and 69.7°, respectively.

Fig. 2b–g shows the 45°-tilted top-view SEM images of ed-Pt, eg-Pt, and sp-Pt films on acid-treated carbon cloth. The morphology of ed-Pt film is particle-like, as shown in Fig. 2b and c. The eg-Pt film exhibits the smoother surface (Fig. 2d and e), similar to sp-Pt film as shown in Fig. 2f and g.

3.3. EIS of Pt/a-CC cathode for MFC

A good cathode for MFC must provide good electrical conduction, i.e. low impedance at 0.1 Hz, which is close to zero frequency in DC measurement for MFC. Fig. 3 shows the impedance of a-CC, ed-Pt/a-CC, eg-Pt/a-CC, and sp-Pt/a-CC measured in LB/DH5α solution by electrochemical impedance spectroscopy (EIS). The interfacial properties between cathode and electrolyte, which play an important role in MFC system, could be determined by EIS measurement over a range of 0.1–100 kHz. Results show that the resistive impedance Z_R (Fig. 3a) was comparable to capacitive impedance Z_C ($Z_C = 1/2\pi fC$, Fig. 3b), where f and C are frequency and capacitance, respectively. It implies that the Pt deposited on carbon cloth as a cathode, no matter by which deposition method, transfers carriers through both resistive conduction and capacitive coupling. The total impedance ($Z = Z_C + Z_R$) per unit area for a-CC and the eg-Pt, sp-Pt, and ed-Pt on carbon cloth are 2604, 2011.5, 1624.6 and 1288.5 Ω/cm^2 at 0.1 Hz, respectively. Fig. 3c shows the results of the frequency versus phase, which all show the phases of about 45° at 0.1 Hz for a-CC, ed-Pt/a-CC, eg-Pt/a-CC, and sp-Pt/a-CC. This confirms again the carriers transfer through both capacitive coupling and resistive conduction [38].

3.4. Performance of MFC with different cathodes and Pt loading

Fig. 4a shows the amount of Pt (Pt loading) deposited on carbon cloth versus power density. From the results, the Pt loading of ed-Pt was 242.04 ± 16.30 μg/cm^2, corresponding to the power density of 59 ± 18 mW/m^2, and those of eg-Pt and sp-Pt were 679.00 ± 42.37 μg/cm^2 and 1589.00 ± 453.91 μg/cm^2 corresponding to their power densities of 8 ± 4 and 3 ± 1 mW/m^2, respectively. The power density manifested by ed-Pt on carbon cloth increases about 7 times and 24 times compared to that by eg-Pt and sp-Pt, respectively. The Pt loading of ed-Pt decreases about 2.8 times and 6.6 times compared to that of eg-Pt and sp-Pt, respectively. According to above results, the ed-Pt reveals the highest power density even with the lowest Pt loading.

Fig. 4b and c shows the power density and polarization curves, respectively, obtained from the MFC system with different Pt/a-CC cathodes. The MFC cathode with ed-Pt shows the highest power density compared to that of eg-Pt and sp-Pt (Fig. 4b). Fig. 4c shows polarization curves with the cell voltage versus current density. Both open circuit voltage (OCV) and current density obtained from the MFC with ed-Pt in cathode are higher than those with eg-Pt and sp-Pt. According to above results, the ed-Pt on carbon cloth as a cathode exhibit the best performance for MFC application.

3.5. Electrochemical characterization of various Pt/a-CC

The Pt on acid-treated carbon cloth was characterized by cyclic voltammogram (CV) with the data taken in the fifth cycles, where a steady state was obtained in the electrolyte of 0.5 M H_2SO_4 solution under Ar atmosphere. The potential was scanned between −0.25 V and 1.0 V (vs. Ag/AgCl) with a scan rate of 50 mV/s at room temperature (RT). Fig. 5a–c shows that the voltammograms of Pt are similar to that of polycrystalline Pt reported [39]. The peaks for hydrogen and oxygen adsorption/desorption on the Pt surface in 0.5 M H_2SO_4 solution can be clearly observed. It is also easy to observe the peaks for hydrogen redox reaction in the region of negative potential (−0.205 to 0.104 V, vs. Ag/AgCl). Besides, the redox reactions of oxygen-like series such as Pt—O and Pt—OH on Pt surface in the positive region (0.645 to −0.014 V, vs. Ag/AgCl) are easily observed [26,39]. For electrochemical performance, the real active surface of Pt on acid-treated carbon cloth (Pt/a-CC) could be estimated from the integrated charge in the hydrogen adsorption region of CV plots (i.e., the hatched areas). The hatched areas

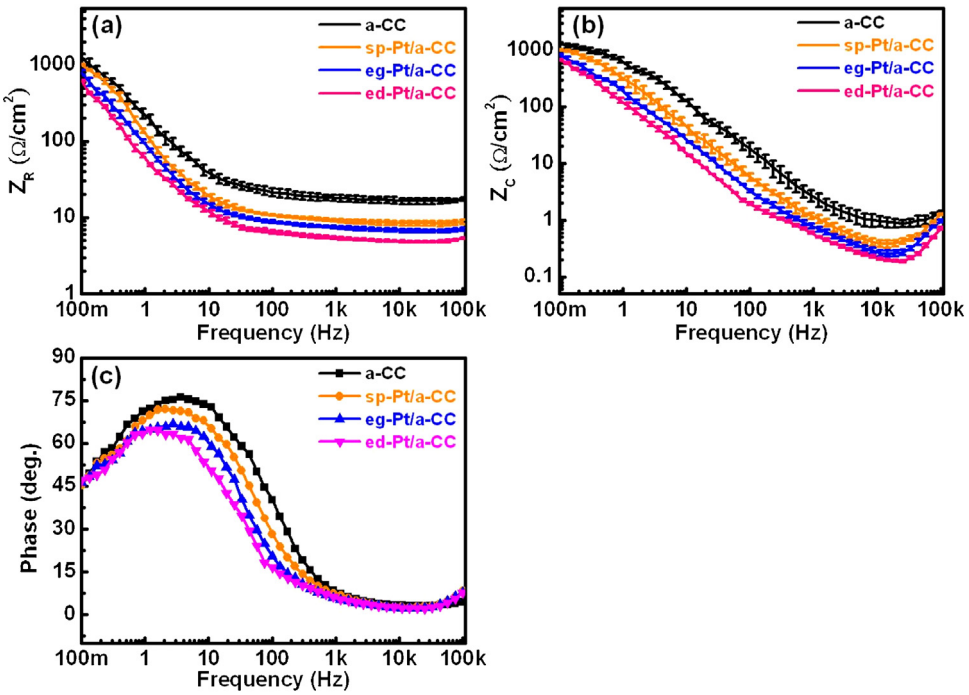

Fig. 3. EIS measurement of the samples with a-CC, and the ed-Pt/a-CC, eg-Pt/a-CC, and sp-Pt/a-CC cathodes were measured to obtain their (a) interfacial resistive impedance, (b) interfacial capacitive impedance, and (c) phase versus frequency.

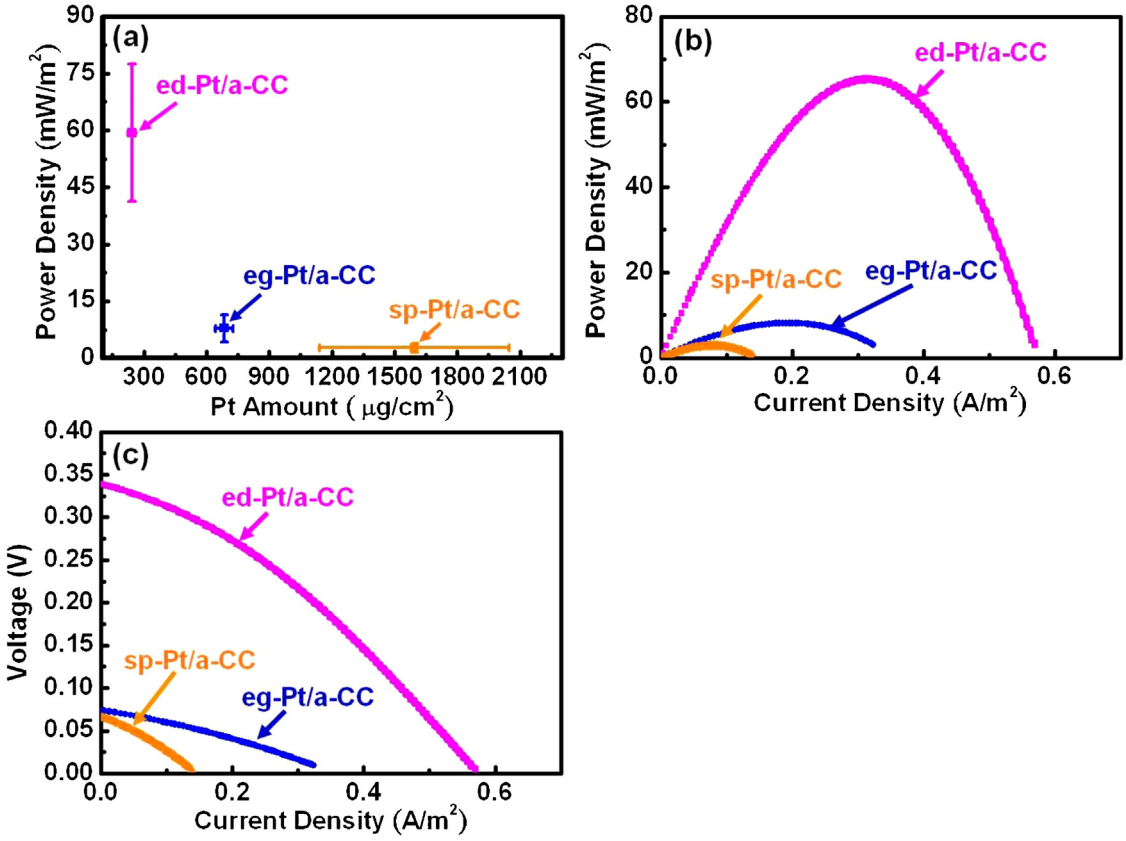

Fig. 4. The polarization curves measured during MFC operation for the samples with ed-Pt/a-CC, eg-Pt/a-CC, and sp-Pt/a-CC cathodes. The (a) power density versus the amount of Pt (Pt loading), (b) power density versus current density, and (C) voltage versus current density.

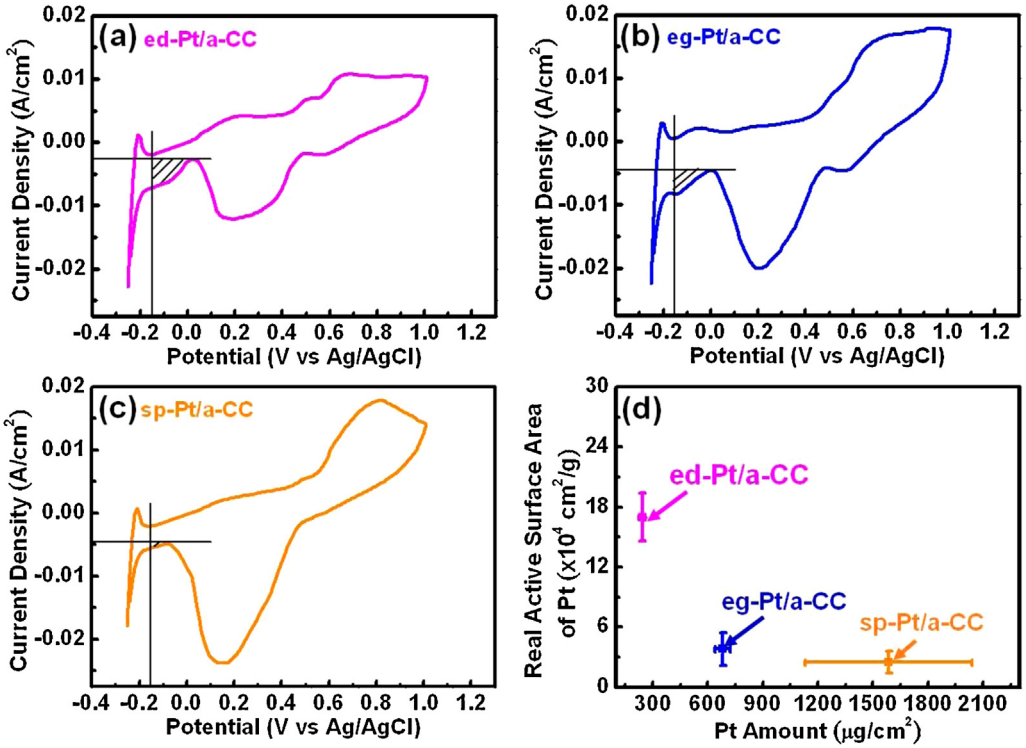

Fig. 5. Cyclic voltammograms (CV) plots for the measurements in 0.5 M H_2SO_4 solution using the samples with (a) ed-Pt/a-CC, (b) eg-Pt/a-CC and (c) sp-Pt/a-CC, with the indication of their respective hatched area related to hydrogen electroabsorption. (d) The real active surface area of Pt per unit area versus Pt amount (Pt loading) for the samples with ed-Pt/a-CC, eg-Pt/a-CC, and sp-Pt/a-CC.

of real active surface of Pt are shown in Fig. 5a–c, and a corresponding value of 0.21×10^{-3} C/cm^2 was calculated with a surface density of 1.3×10^{15} atoms/cm^2 (the typical value of polycrystalline Pt) [39,40] and the areas of active surface were calculated from the following formula:

$$\mathrm{AEL}(\mathrm{cm}^2/\mathrm{g}) = \frac{\mathrm{QH}(\mathrm{C})}{(0.21 \times 10^{-3}\,\mathrm{C/cm}^2) \times \mathrm{Pt\ loading}\,(\mathrm{g})}$$

where AEL is the real active surface for per gram of the Pt obtained by electrochemical method of catalyst (in the unit of cm^2/g), and QH is the charge exchanged during the electroadsorption of hydrogen on Pt. All measurements were conducted with nearly the same area of electrode (~1 cm^2). Fig. 5d shows the real active surface area of the Pt deposited by different methods versus their respective Pt loading. The average real active surface areas of ed-Pt, eg-Pt, and sp-Pt are 17×10^4, 3.82×10^4, and 2.47×10^4 cm^2/g, respectively, i.e., the area for ed-Pt is about 4.5 times larger than that of eg-Pt, and 6.9 times larger than that of sp-Pt. The deviation of surface area analyses depends on deposition methods and the roughness of micro-scale carbon cloth. The ed-Pt is deposited by the solution process with a high coverage of nanoparticles deposited on carbon cloth. The Pt nanoparticles can be deposited mostly on the whole carbon cloth. Compared to ed-Pt, the eg-Pt and sp-Pt were deposited by the diffusion of Pt ions onto carbon cloth, with a smoother and denser film properties (See Fig. 2g–d). Besides, their film coverage was lower than that of ed-Pt. Therefore, the deviation of surface area measurement in eg-Pt and sp-Pt are smaller than ed-Pt. However, the ed-Pt could be well dispersed and exhibited the highest amount of Pt (0) (see Table 1) to achieve the highest performance of MFC. Furthermore, the power density in ed-Pt increased at least 4 times compared to that of eg-Pt and sp-Pt at least. The results show that the performance in ed-Pt is always higher than that of eg-Pt and sp-Pt.

4. Conclusions

In summary, the improvement of catalytic efficiency was obtained by electrodepsited-Pt on carbon cloth as a cathode in MFC system. The highest quantity of Pt (0) has been obtained from the Pt deposited on acid-treated carbon cloth by electrodeposition from XPS analysis compared to that deposited by e-gun and sputtering. According to the catalytical effect of Pt, Pt (0) exhibits the highest active efficiency for hydrogen electroabsorption. From the EIS measurement, the impedance of Pt deposited by electrodeposition is lower than that of Pt deposited by e-gun and sputtering. From CV measurements, the results show that the real active surface area of Pt deposited by electrodeposition is higher than that of Pt deposited by e-gun and sputtering. Besides, the highest power density was achieved for the MFC with electrodeposited Pt, even it contained the smallest Pt loading compared to eg-Pt and sp-Pt. Because the Pt deposited on carbon cloth by electrodeposition as a cathode exhibits the highest power density (even with the lowest Pt loading), highest active surface area, and highest active efficiency compared to those by e-gun and sputtering, it shows the highest potential for MFC applications.

Acknowledgments

This work was supported by National Science Council under project number NSC98-2627-E-007-001. The authors would like to thank Prof. Peng's team at NCTU for providing bacteria culture system, as well as Dr. Ming-Chi Tsai at NTHU for electrodeposition system, Prof. Yu-Luen Chueh's Lab in the department of

MSE at NTHU (NTHU-MSE) for the support of e-gun system and Prof. Tai-Bor Wu's Lab at NTHU-MSE for the support of sputtering system.

Appendix A. Supplementary data

Supplementary data associated with this article can be found, in the online version, at http://dx.doi.org/10.1016/j.electacta.2013.06.019.

References

[1] J.C. Biffinger, J. Pietron, R. Ray, B. Little, B.R. Ringeisen, A biofilm enhanced miniaturemicrobial fuel cell using *Shewanella oneidensis* and oxygen reduction cathodes, Biosensors and Bioelectronics 22 (2007) 1672.
[2] A. Dumitru, A. Morozan, M. Ghiurea, K. Scott, S. Vulpe, Biofilm growth from wastewater on MWNTs and carbon aerogels, Physica Status Solidi (a) 205 (2008) 1484.
[3] C. Feng, L. Ma, F. Li, H. Mai, X. Lang, S. Fan, A polypyrrole/anthraquinone-2,6-disulphonic disodium salt (PPy/AQDS)-modified anode to improve performance of microbial fuel cells, Biosensors and Bioelectronics 25 (2010) 1516.
[4] P. Liang, H. Wang, X. Xia, X. Huang, Y. Mo, X. Cao, M. Fan, Carbon nanotube powders as electrode modifier to enhance the activity of anodic biofilm in microbial fuel cells, Biosensors and Bioelectronics 26 (2010) 3000.
[5] S. Cheng, B.E. Logan, Ammonia treatment of carbon cloth anodes to enhance power generation of microbial fuel cells, Electrochemistry Communications 9 (2007) 492.
[6] B.E. Logan, Exoelectrogenic bacteria that power microbial fuel cells, Nature Reviews Microbiology 7 (2009) 375.
[7] H. Rismani-Yazdi, S.M. Carver, A.D. Christy, O.H. Tuovunen, Cathodic limitations in microbial fuel cells: an overview, Journal of Power Sources 180 (2008) 683.
[8] X. Wang, S. Cheng, X. Zhang, X.Y. Li, B.E. Logan, Impact of salinity on cathode catalyst performance in microbial fuel cells (MFCs), International Journal of Hydrogen Energy 36 (2011) 13900.
[9] M. Zhou, M. Chi, J. Luo, H. He, T. Jin, An overview of electrode materials in microbial fuel cells, Journal of Power Sources 196 (2011) 4427.
[10] L. Birry, P. Mehta, F. Jaouen, J.P. Dodelet, S.R. Guiot, B. Tartakovsky, Application of iron-based cathode catalysts in a microbial fuel cell, Electrochimica Acta 56 (2011) 1505.
[11] L. Wang, P. Liang, J. Zhang, X. Huang, Activity and stability of pyrolyzed iron ethylenediaminetetraacetic acid as cathode catalyst in microbial fuel cells, Bioresource Technology 102 (2011) 5093.
[12] N. Duteanu, B. Erable, S.M. Senthil Kumar, M.M. Ghangrekar, K. Scott, Effect of chemically modified Vulcan XC-72R on the performance of air-breathing cathode in a single-chamber microbial fuel cell, Bioresource Technology 101 (2010) 5250.
[13] F. Zhang, S. Cheng, D. Pant, G.V. Bogaert, B.E. Logan, Power generation using an activated carbon and metal mesh cathode in a microbial fuel cell, Electrochemistry Communications 11 (2009) 2177.
[14] Y. Zhang, G. Mo, X. Li, J. Ye, Iron tetrasulfophthalocyanine functionalized graphene as a platinum-free cathodic catalyst for efficient oxygen reduction in microbial fuel cells, Journal of Power Sources 197 (2012) 93.
[15] L. Zhang, C. Liu, L. Zhuang, W. Li, S. Zhou, J. Zhang, Manganese dioxide as an alternative cathodic catalyst to platinum in microbial fuel cells, Biosensors and Bioelectronics 24 (2009) 2825.
[16] M. Mahmmoud, T.A. Gad-Allah, K.M. El-Khatib, F. El-Gohary, Power generation using spinel manganese–cobalt oxide as a cathode catalyst for microbial fuel cell applications, Bioresource Technology 102 (2011) 10459.
[17] S. Hrapovic, M.F. Manuel, J.H.T. Luong, S.R. Guiot, B. Tartakovsky, Electrodeposition of nickel particles on a gas diffusion cathode for hydrogen production in a microbial electrolysis cell, International Journal of Hydrogen Energy 35 (2010) 7313.
[18] P.A. Selembo, M.D. Merrill, B.E. Logan, Hydrogen production with nickel powder cathode catalysts in microbial electrolysis cells, International Journal of Hydrogen Energy 35 (2010) 428.
[19] J. Liu, Y. Feng, X. Wang, Q. Yang, X. Shi, Y. Qu, N. Ren, The effect of water proofing on the performance of nickel foam cathode in microbial fuel cells, Journal of Power Sources 198 (2012) 100.
[20] J.R. Kim, J.Y. Kim, S.B. Han, K.W. Park, G.D. Saratale, S.E. Oh, Application of Co-naphthalocyanine (CoNPc) as alternative cathode catalyst and support structure for microbial fuel cells, Bioresource Technology 102 (2011) 342.
[21] E.H. Yu, S. Cheng, K. Scott, B.E. Logan, Microbial fuel cell performance with non-Pt cathode catalysts, Journal of Power Sources 171 (2007) 275.
[22] B. Erable, L. Etcheverry, A. Bergel, Increased power from a two-chamber microbial fuel cell with a low-pH air-cathode compartment, Electrochemistry Communications 11 (2009) 619.
[23] V. Neburchilov, P. Mehta, A. Hussain, H. Wang, S.R. Guiot, B. Tartakovsky, Microbial fuel cell operation on carbon monoxide: cathode catalyst selection, International Journal of Hydrogen Energy 36 (2011) 11929.
[24] E. Martin, B. Tartakovsky, O. Savadogo, Cathode materials evaluation in microbial fuel cells: a comparison of carbon, Mn_2O_3, Fe_2O_3 and platinum materials, Electrochimica Acta 58 (2011) 58.
[25] M.C. Tsai, T.K. Yeh, C.H. Tsai, Methanol oxidation efficiencies on carbon-nanotube-supported platinum and platinum–ruthenium nanoparticles prepared by pulsed electrodeposition, International Journal of Hydrogen Energy 36 (2011) 8261.
[26] M.C. Tsai, T.K. Yeh, C.Y. Chen, C.H. Tsai, A catalytic gas diffusion layer for improving the efficiency of a direct methanol fuel cell, Electrochemistry Communications 9 (2007) 2299.
[27] H.J. Ahn, J.H. Lee, Y. Jeong, J.H. Lee, C.S. Chi, H.J. Oh, Nanostructured carbon cloth electrode for desalination from aqueous solutions, Materials Science and Engineering: A 449–451 (2007) 841–845.
[28] H.J. Oh, J.H. Lee, H.J. Ahn, Y. Jeong, Y.J. Kim, C.S. Chi, Nanoporous activated carbon cloth for capacitive deionization of aqueous solution, Thin Solid Films 515 (2006) 220.
[29] M. Polovina, B. Babic, B. Kaluderovic, A. Dekanski, Surface characterization of oxidized activated carbon cloth, Carbon 35 (1997) 1047.
[30] Z. Liu, J.Y. Lee, M. Han, W. Chen, L.M. Gan, Synthesis and characterization of PtRu/C catalysts from microemulsions and emulsions, Journal of Materials Chemistry 12 (2002) 2453.
[31] C.R. Parkinson, M. Walker, C.F. McConville, Reaction of atomic oxygen with a Pt(1 1 1) surface: chemical and structural determination using XPS, CAICISS and LEED, Surface Science 545 (2003) 19.
[32] X. Zhang, K.Y. Chan, Water-in-oil microemulsion synthesis of platinum–ruthenium nanoparticles, their characterization and electrocatalytic properties, Chemistry of Materials 15 (2003) 451.
[33] S.R. De Miguel, O.A. Scelza, M.C. Roman-Martinez, C. Salinnas-Martinez de Lecea, D. Cazorla-Amoros, A. Linares-Solano, States of Pt in Pt/C catalyst precursors after impregnation, drying and reduction steps, Applied Catalysis A: General 170 (1998) 93.
[34] A.K. Shukla, M. Neergat, P. Bera, V. Jayaram, M.S. Hegde, An XPS study on binary and ternary alloys of transition metals with platinized carbon and its bearing upon oxygen electroreduction in direct methanol fuel cells, Journal of Electroanalytical Chemistry 504 (2001) 111.
[35] A.S. Arico, A.K. Shukla, H. Kim, S. Park, M. Min, V. Antonucci, An XPS study on oxidation states of Pt and its alloys with Co and Cr and its relevance to electroreduction of oxygen, Applied Surface Science 172 (2001) 33.
[36] N.H. Li, S.G. Sun, S.P. Chen, Studies on the role of oxidation states of the platinum surface in electrocatalytic oxidation of small primary alcohols, Journal of Electroanalytical Chemistry 430 (1997) 57.
[37] H. Yoshida, Y. Yazawa, T. Hattori, Effects of support and additive on oxidation state and activity of Pt catalyst in propane combustion, Catalysis Today 87 (2003) 19.
[38] H.C. Su, C.M. Lin, S.J. Yen, Y.C. Chen, C.H. Chen, S.R. Yeh, W.L. Fang, H. Chen, D.J. Yao, Y.C. Chang, T.R. Yew, A cone-shaped 3D carbon nanotube probe for neural recording, Biosensors and Bioelectronics 26 (2010) 220.
[39] Z. Liu, J.Y. Lee, W. Chen, M. Han, L.M. Gan, Physical and electrochemical characterizations of microwave-assisted polyol preparation of carbon-supported PtRu nanoparticles, Langmuir 20 (2004) 181.
[40] Z. Liu, L.M. Gan, L. Hong, W. Chen, J.Y. Lee, Carbon-supported Pt nanoparticles as catalysts for proton exchange membrane fuel cells, Journal of Power Sources 139 (2005) 73.